Volume 14, Issue 1, 142402 (1-10)

Iranian Journal of Catalysis (IJC)

https://doi.org/10.57647/j.ijc.2024.1401.02

Synthesis of new magnetic reusable oil sorbent catalysts based on dodecanol and dodecyl sulfate: their application for oil/water separation

Negar Zekri, Reza Fareghi-Alamdari*

Faculty of Chemistry & Chemical Engineering, Malek-Ashtar University of Technology, Tehran, Iran.

***Corresponding author:** reza_fareghi@yahoo.com,reareghialamdari@mut.ac.ir

Original Research

Received:
4 October 2023
Revised:
29 December 2023
Accepted:
10 January 2024
Published online:
20 March 2024

Abstract:

Magnetic nanoparticles (MNPs) were treated with dodecyl sulfate (DS) and dodecanol (DO) to enhance their affinity for lipids. Various methods, such as X-ray powder diffraction (XRD), scanning electron microscopy (SEM), vibrating sample magnetometery (VSM), thermal gravimetric analysis (TGA), and FTIR spectroscopy were employed to analyze and characterize these modified MNPs. The functionalized MNPs were employed to adsorb different types of oils (edible, motor, and diesel oils). MNP@DO and MNP@DS exhibited oil absorption capacities of up to three and two times their own mass for edible oil, respectively. The complete repulsion of water was evident, and a rapid interaction between lipophilic magnetic catalysts and oil on the water's surface was observed. These oil-absorbing catalysts could be efficiently removed by employing an external magnet, and they demonstrated excellent reusability. The findings indicate that these novel catalysts exhibit substantial oil-absorbing capabilities and can be used as low-cost and effective technique for oil/solvent-spill cleanups.

Keywords: Oil sorbent catalysts; Oil spill cleanup; Functionalized magnetic nanoparticles; Magnetic sorbent catalysts

1. Introduction

The industrial significance of oil spills and chemical leaks has grown markedly in recent years, causing substantial concern [1–6]. This issue is one of the most considerable warnings to the coastal environment and oceanic ecosystem, having serious risks for aquatic organisms and humans [7]. Stopping this trend is very difficult due to the exploration, production, and utilization of a large amount of oil in the year and the uncontrolled release of oils during transportation or storage steps [8]. To resolve this global problem, several mechanical, physical, and chemical techniques have been developed. These methodologies are used to collect and separate oil pollutants from water surfaces. The majority of these approaches rely on adsorbent materials for oil/water separation, utilizing a range of adsorptive substances like zeolites, activated carbon, wool, nanocomposite membranes, and exfoliated graphite [6, 9–15]. The challenge on the design of sorbent materials resulted from some drawbacks associated with them, including low adsorption capability, poor permanence and less selective water/oil absorption, and difficult removal of the sorbent from water [16–20]. Given the modest adsorption capacity of these introduced sorbent materials, enhancing their reusability emerges as a crucial factor in improving the oil/water separation capabilities of these engineered materials.

Magnetic nanoparticles are good candidates to be used as reusable oil and heavy metal adsorbent materials, and numerous types of magnetic compounds designed for this purpose have been documented in the literature [20–26]. In this way, magnetic superhydrophobic particles can be placed on the contaminated water region and next be removed using an external magnetic field. Furthermore, the excellent monodispersibility of superhydrophobic magnetic particles on water surfaces broadens their potential for large-scale applications. For instance, Mao et al. reported the development of MNPs-modified polymer microspheres that could be used for oil removal in aqueous environments [20].

Zhuo et al. created a magnetic aerogel composite comprising polystyrene, Fe_3O_4, and grapheme [21]. Wu et al. successfully synthesized a magnetic nanofibrous composite mat composed of polystyrene and polyvinylidene fluoride nanofibers with selective incorporation of MNPs, which was employed for oil removal from water [24]. Additionally, a superhydrophobic magnetic cellulose sponge was prepared for oil removal from water [19], while Du and colleagues reported the development of an ultra-thermostable, magnetic-driven, and superhydrophobic quartz fiber for water remediation [25].

In continuation of our program on the synthesis of magnetic nanoparticle functionalized catalysts [27–30], here we report a facile approach for preparing two new, magnetic, reusable, and superhydrophobic catalysts to be used as oil-adsorbents for application in removing of oils from the water surface. The findings indicate that using these catalysts can be a low-cost and effective technique for oil/solvent spill cleanups.

2. Materials and methods

All solvents and chemicals used in this study were procured from the Merck chemical company. The specification of the used oils are: Edible oil: (Sun flower oil, food grade, viscosity @ 25 °C: $30-32$ cSt); Motor oil: Caspian Motor Oil 20W50 SL/CF4 (viscosity @100 °C: $20-21.5$ cSt, Density @15 °C: 0.881 g/cm^3); Diesel oil: Caspian diesel oil SAE 15W40 API CI-4 (viscosity @100 °C: 15.7 cSt, Density @15 °C: 0.875 g/cm^3). All of the materials were used without further purification.

2.1 Equipment

FT-IR spectra were obtained using KBr pellets and recorded on a Nicolet-860 spectrometer. Thermal gravimetric analyses were conducted using a Perkin Elmer thermal analysis instrument. Magnetic measurements of the sorbents were performed using a vibrating sample magnetometer (VSM) with a 4-inch sample holder from Daghigh Meghnatis Kashan Company, Iran, at room temperature. The chemical and elemental compositions of the sorbents were assessed using scanning electron microscopy (VEGA 3 TESCAN) equipped with an Oxford Instruments X-MAX 50 EDS system. X-ray powder diffraction (XRD) was carried out using a Philips X′ Pert diffractometer with Co$K\alpha$ radiation. The specific surface area of the adsorbent materials was determined by the Brunauer-Emmett-Teller (BET) method using a Micrometrics Tristar II 3020 instrument.

2.2 Preparation of sorbents

2.2.1 Synthesize of Fe_3O_4@SiO_2

Fe_3O_4@SiO_2 was synthesized according to the reported procedure [31]. $FeCl_3$ (1.70 g, 10 mmol), $FeCl_2\cdot{}_4H_2O$ (1 g, 5 mmol), and 12.7 mL of 0.4 M HCl were dissolved in 125 mL of 0.7 M NH_3 solution, which was continuously purged with N_2 gas. This dissolution process took place in an ultrasonic bath under an N_2 atmosphere, at a temperature of 25 °C for a duration of 20 minutes. The resulting precipitate was subjected to three wash cycles with deionized water using an ultrasonic bath. Subsequently, 50 mL of deionized water were added to the precipitate, followed by the introduction of 250 mL of 2-propanol into this suspension within the ultrasonic bath for 20 minutes. Next, 11.85 mL of polyethylene glycol 400, 50 mL of deionized water, 25 mL of NH_3 (28%), and 3 mL of tetraethyl orthosilicate (TEOS) were sequentially added. The reaction mixture was agitated for a period of 24 hours at 25 °C using a mechanical shaker. Finally, the magnetic Fe_3O_4@SiO_2 nanoparticles were isolated using a magnetic magnet, followed by multiple rinses with deionized water and ethanol. The collected nanoparticles were then dried under vacuum at 70 °C, resulting in the production of Fe_3O_4@SiO_2 in the form of a black solid.

2.2.2 Synthesize of Fe_3O_4@SiO_2@Cl

To synthesize this material, the previously prepared Fe_3O_4@SiO_2 nanoparticles (2 g) were dispersed in 60 mL of thionyl chloride ($SOCl_2$) for 30 minutes. Subsequently, the mixture was refluxed for duration of 3 hrs. Finally, the chloro-functionalized magnetic nanoparticles were obtained in the form of a black solid after drying in a vacuum oven.

2.2.3 Synthesize of Fe_3O_4@SiO_2@DS (MNP@DS)

To synthesize MNP@DS, the freshly prepared Fe_3O_4@SiO_2@Cl (2 g), together with sodium dodecyl sulfate (0.57 g, 2 mmol) and 0.5 mL of triethylamine, were dissolved in 5 mL dried toluene. The resulting solution was then refluxed for a duration of 24 hours at a temperature of 110 °C. The resulting precipitate was subjected to several wash cycles using toluene and subsequently dried in a vacuum oven. Following this, it underwent multiple rinses with water and was once again dried in a vacuum oven. The final product was obtained in the form of a dark solid.

2.2.4 Synthesize of Fe_3O_4@SiO_2@DO (MNP@DO)

The procedure for synthesizing MNP@DO is the same as for MNP@DS. Specifically, the freshly prepared Fe_3O_4@SiO_2@Cl (2 g), along with 0.5 mL dodecanol and 0.5 mL of triethylamine, were dissolved in 5 mL dried toluene. This mixture was then refluxed for duration of 24 hours at a temperature of 110 °C. The resulting precipitate was subjected to several wash cycles using toluene and subsequently dried in a vacuum oven. Following this, the solid was rinsed multiple times with water and once again dried in a vacuum oven. The final product was obtained in the form of a black solid.

2.3 Sorption experiments

The oil adsorbent capacity of the samples was assessed through weight measurements. Initially, each sample was weighed (m_1). In the subsequent step, three different types of oils were introduced onto the water surface in separate beakers. Subsequently, the samples were added to the respective beakers. After a 10-minute period, the samples that had adsorbed the oil were removed from the beakers using a magnet, and their mass was determined (m_2).

The sorption capacity (k) of each sample was calculated using the following formula:

$$k = (m_2 - m_1)/m_1$$

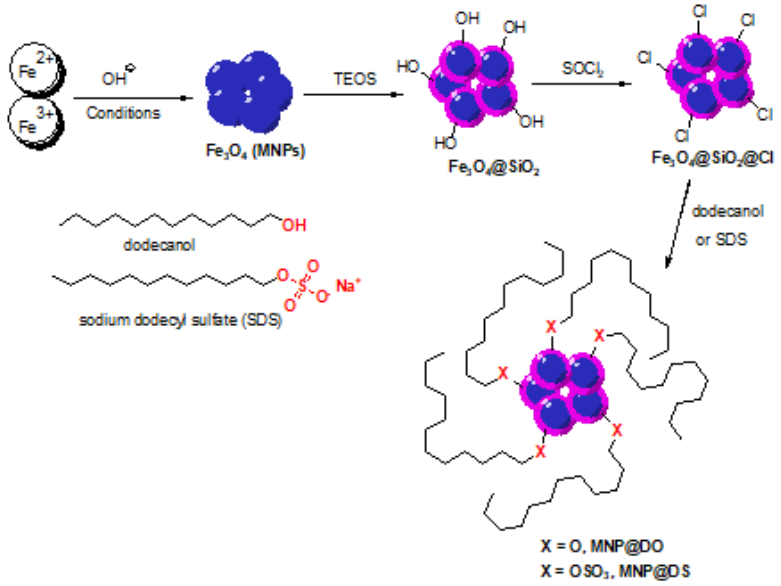

Scheme 1. Synthesis process for the preparation of MNP@DS and MNP@DO nanomaterials.

This adsorption experiment was conducted a total of 10 times for each sample. After each adsorption cycle, the oil-adsorbed samples were thoroughly washed with toluene multiple times and then dried in a vacuum oven.

3. Results and discussion

3.1 Synthesis and characterization of MNP-supported dodecyl sulfate (MNP@DS) and MNP-supported dodecanol (MNP@DO)

The schematic representation of the synthesis process for the preparation of MNP@DS and MNP@DO materials has been illustrated in Scheme 1.

Magnetic nanoparticles were synthesized using a co-deposition procedure [31]. These nanoparticles were then coated with a silica layer through a sol-gel process to create core-shell magnetic nanoparticles (Fe_3O_4@SiO_2). This silica layer serves the dual purpose of preventing the aggregation of the magnetic core and facilitating surface functionalization. It offers Si−OH groups on the surface of the nanoparticles, allowing for precise chemical modification. Subsequently, the Fe_3O_4@SiO_2 substrate underwent treatment with thionyl chloride ($SOCl_2$) to yield a chlorine-functionalized magnetic nanoparticle substrate denoted as Fe_3O_4@SiO_2@Cl [30]. The reaction between sodium dodecyl sulfate or dodecanol and Fe_3O_4@SiO_2@Cl resulted in the production of two catalysts: MNP-supported dodecyl sulfate (MNP@DS) and MNP-supported dodecanol (MNP@DO).

Subsequently, these materials were characterized using various analytical techniques, which included FT-IR, SEM, EDX, VSM, BET, and TGA-DTG.

To investigate the successful functionalization of the MNPs, FT-IR was employed. Figure 1 illustrates a comparison of the FT-IR spectra among Fe_3O_4@SiO_2, Fe_3O_4@SiO_2@Cl, MNP@DO, and MNP@DS.

In the FT-IR spectrum of Fe_3O_4@SiO_2 (Fig. 1a), notable

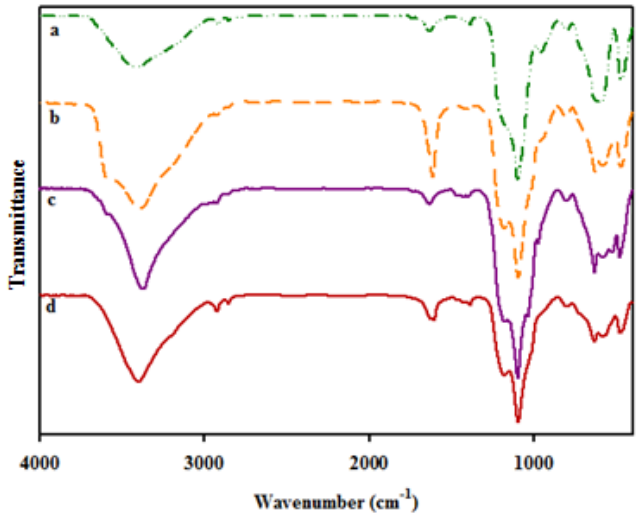

Figure 1. The FT-IR spectra of Fe_3O_4@−SiO_2 (a), Fe_3O_4@−SiO_2@Cl (b), MNP@DS (c), MNP@DO (d).

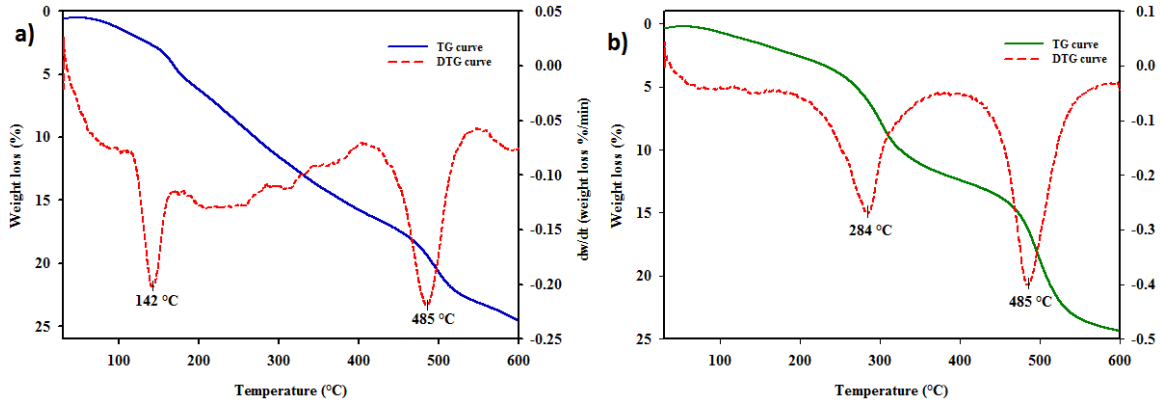

Figure 2. The TGA-DTG curves of MNP@DO (a) and MNP@DS (b).

adsorption peaks are observed. The peak at 624 cm^{-1} can be attributed to the vibration of the Fe−O bond in the tetrahedral site of the bare magnetic microspheres [32]. The broad band at 3430 cm^{-1} corresponds to the O−H stretching vibration originating from O−H bonds. The presence of the silica layer on the MNPs' surface is confirmed by two distinct bands at 1096 cm^{-1} and 958 cm^{-1}, which are associated with the symmetrical and asymmetrical vibrations of the Si−O−Si bonds [32]. Moving on to the FT-IR spectrum of Fe_3O_4@SiO_2@Cl (Fig. 1b), the appearance of a vibration band at 579 cm^{-1} indicates the presence of Si−Cl bonds [30]. Other peaks related to Fe_3O_4@SiO_2 are observed with slight shifts due to changes in the chemical environment.

In the FT-IR spectrum of MNP@DS (Fig. 1c), in addition to the fundamental peaks, new peaks associated with aliphatic C−H bond stretching are observed in the range of 2800 – 2900 cm^{-1}. A peak at 1037 cm^{-1} can be attributed to the S=O bond in the SDS chain [33]. In the case of the FT-IR spectrum of MNP@DO (Fig. 1d), upon linking dodecanol to the magnetic nanoparticle surface, a prominent absorption peak of C−H stretching is observed at 2924 cm^{-1} and 2874 cm^{-1}. Additionally, the suppression of certain peaks at lower frequencies suggests that the organic chain is chemically bonded to the surface of the magnetic nanoparticles.

The TGA and DTG curves of MNP@DO and MNP@DS materials are shown in Figure 2.

The thermogram analysis of MNP@DO and MNP@DS materials reveals distinct weight loss patterns at various temperature ranges. A reduction in weight percentage of MNP@DO (Fig 2a) at approximately 120 °C, attributed to absorbed water within the material's structure. Another weight decrease is observed in the range of 140 – 180 °C, indicating the removal of crystalline water from the template of the magnetic nanoparticles. Significant weight losses occur between 220 and 490 °C, linked to the decomposition of grafted organic moieties on the magnetic nanoparticles' surface. This portion of the thermogram indirectly estimates the amount of connected organic material and suggests that approximately 19% (w/w) of dodecanol is grafted onto the MNPs' surface. The weight loses at higher temperature is related to the decomposition of the MNP support. Furthermore, the thermogram analysis for MNP@DS reveals an initial weight loss at approximately 195 °C due to the removal of adsorbed water, accounting for approximately 3.4% of the total weight. A subsequent weight reduction in the range of 195 – 403 °C is associated with the de-

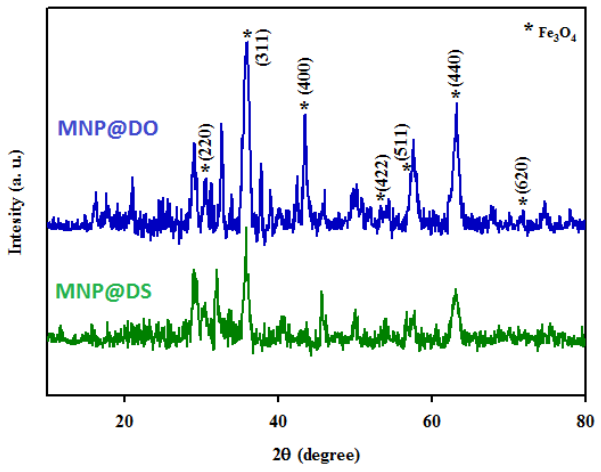

Figure 3. The XRD patterns of MNP@DO and MNP@DS catalysts.

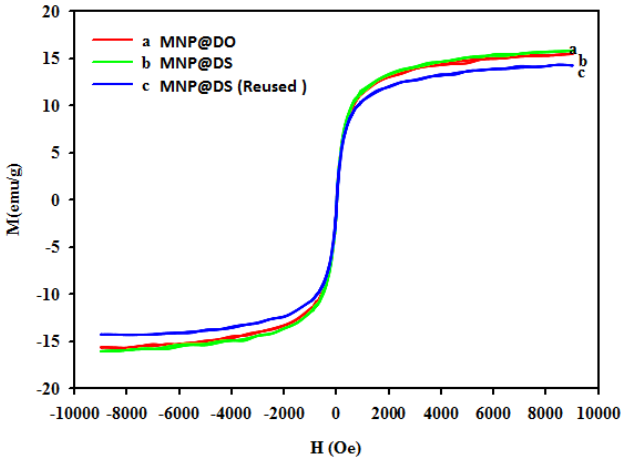

Figure 4. (a) Magnetization curves obtained by VSM for MNP@DO, (b) MNP@DS and (c) reused MNP@DS.

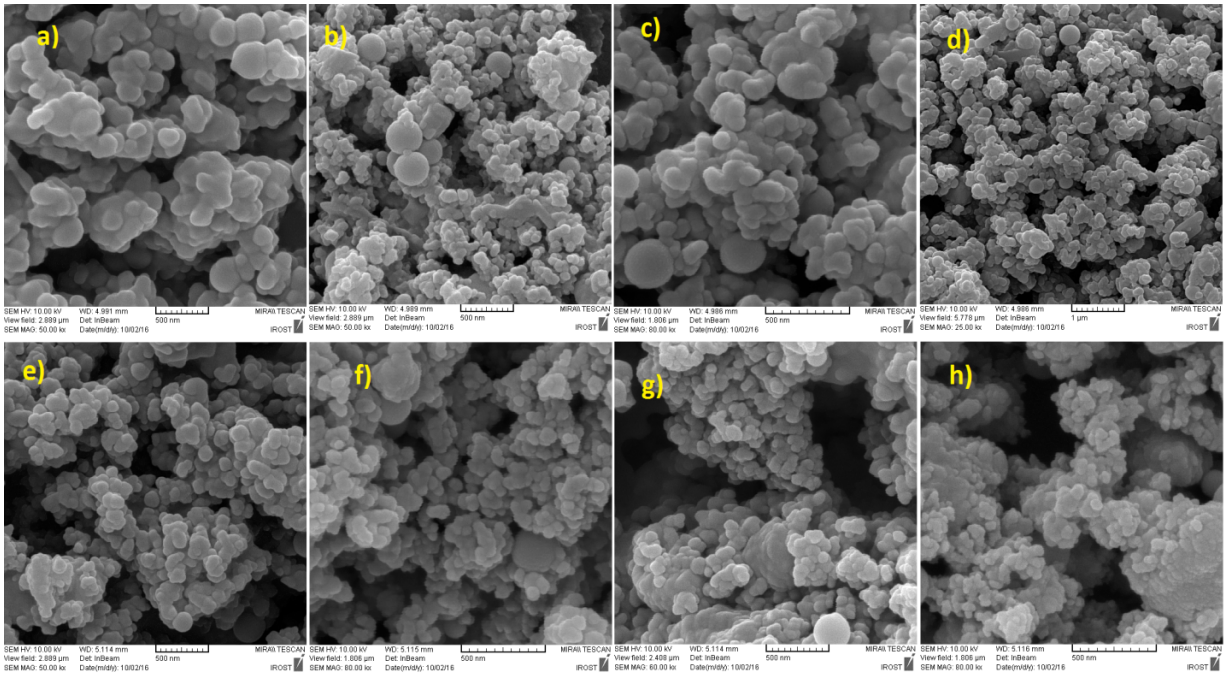

Figure 5. The SEM images of MNP@DO (a-d) and MNP@DS (e-h) with different magnification.

composition of the grafted organic layer from the MNP substrate, indicating an estimated content of approximately 10% (w/w) of supported SDS on the MNPs. The weight decrease at 405 – 600 °C is related to the decomposition of the remaining carbon chains from the MNPs' surface. These observations highlight the high thermal stability of MNP@DO and MNP@DS materials and support the notion of covalent bonding between these groups and the MNPs' surface.

Overall, the observed removal of grafted organic groups at elevated temperatures serves as strong evidence of the remarkable thermal stability exhibited by MNP@DO and MNP@DS materials. This observation strongly supports the concept of covalent bonding between these groups and the surface of the magnetic nanoparticles.

In order to investigate crystallinity, phase composition, and the purity of the synthesized materials, as well as to confirm their structural modifications, powder X-ray diffraction (XRD) studies were conducted (Fig. 3).

The XRD patterns of both MNP@DO and MNP@DS (Fig. 3) exhibit the characteristic peaks of magnetic nanoparticles, indicating the preservation of the crystalline phase stability of the nanoparticles during subsequent surface modifications. As depicted in Figure 3, the reflection planes corresponding to (220), (311), (400), (422), (511), and (440) at 2θ values of 30.3 °C, 35.7 °C, 43.4 °C, 53.1 °C, 57.3 °C, and 63.0 °C, respectively, closely match the face-centered cubic Fe_3O_4 structure (JCPDS Card no. 19-0629) [31]. The reflection plan for the silica layer, which should appear in the range of 2θ = 25 °C, perhaps due to the functionalization of the surface with an organic layer, showed a high intensity.

The magnetization properties of both MNP@DO and MNP@DS materials were examined using a vibrating sample magnetometer (VSM) at room temperature under an applied magnetic field ranging from -9000 to +9000 Oe (Figure 4). As shown in Figure 4, the values of the saturation magnetization are 16 emu g^{-1} for MNP@DO and 15

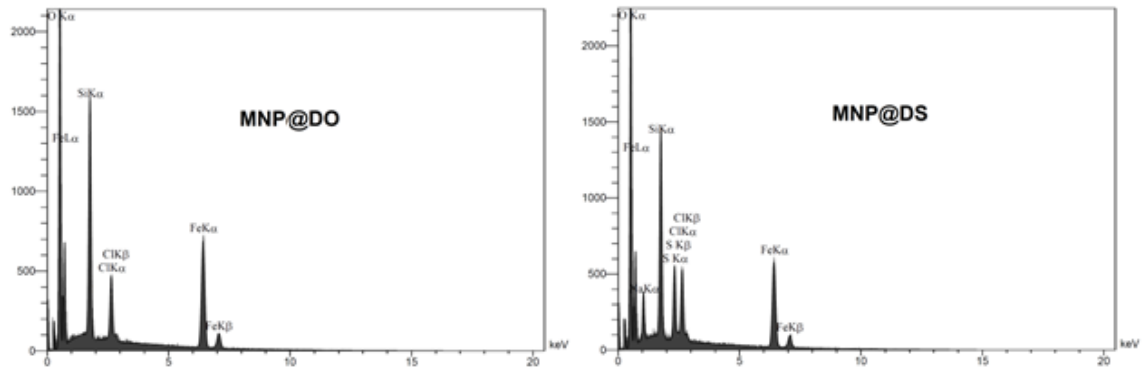

Figure 6. The EDX analysis of (a) the MNP@DO and (b) the MNP@DS.

Table 1. Textural properties of the synthesized nanomaterials.

Entry	Sample	Surface area (m^2/g)	Pore diameter (nm)
1	MNP@DO	112.4	10.61
2	MNP@DS	117.1	8.22

emu g^{-1} for MNP@DS. This slight decrease in saturation magnetization can be attributed to the presence of the organic layer immobilized on the surface of both materials, in contrast to the original Fe_3O_4 nanoparticles [30]. However, despite this decline in the saturation magnetization, the materials can still be competently and easily removed from solution media using an external magnetic field.

The SEM images of MNP@DO and MNP@DS at varying magnifications are illustrated in Figure 5. The SEM images provide a detailed view of the surface morphology of the catalysts, revealing that the nanoparticles exhibit a nearly spherical shape.

The elemental composition of both MNP@DO and MNP@DS were determined through EDX analysis, as shown in Figure 6.

The results depicted in Figure 6a, reveal that the MNP@DO material comprises elements C, O, Si, and Fe. Similarly, MNP@DS contains elements C, O, S, Si, and Fe. Based on the measured content of carbon (C), which accounts for 16.76%, it is possible to calculate the quantity of grafted dodecanol on the surface of magnetic nanoparticles in MNP@DO, amounting to 1.16 mmol.g^{-1} of the material. In the case of MNP@DS, the quantity of dodecyl sulfate was also estimated, and it is approximately 1.13 mmol.g^{-1} of material, determined from the percentage of sulfur (S), which constitutes 3.64% of the composition.

Also, the elemental analysis of the MNP@DS demonstrates the presence S atom with wt% of 3.51. Accordingly, it is

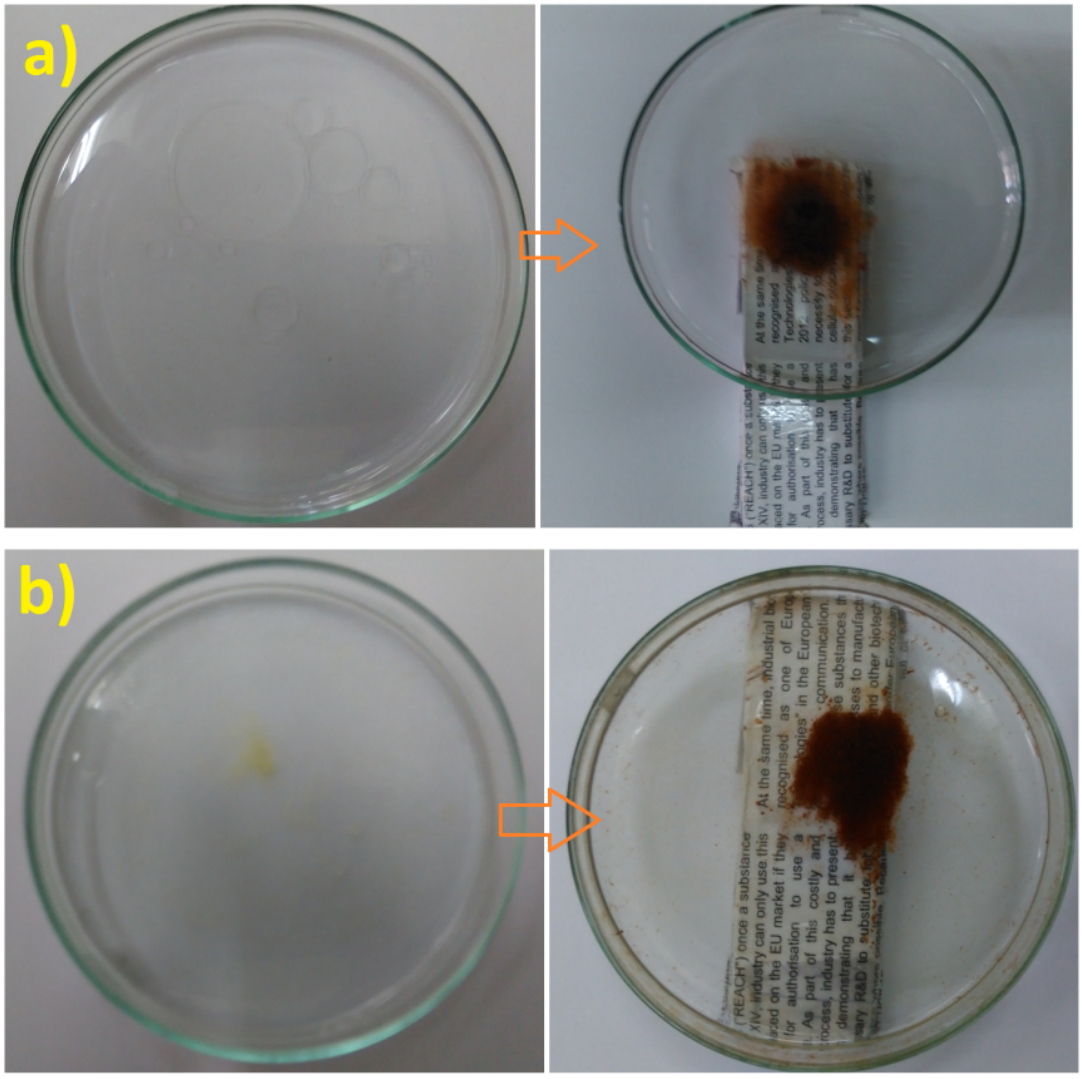

Figure 7. The adsorption of oil from water surface using magnetic sorbent materials. a) Pure oil on water surface (left) and added MNP@DS after 30s (right). b) Pure oil on water surface (left) and added MNP@DO after 30s (right).

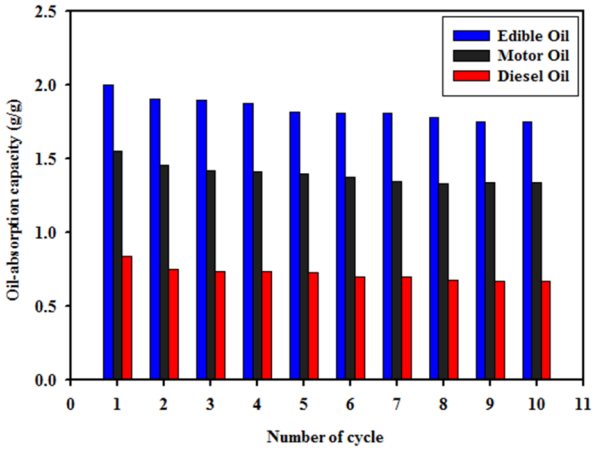

Figure 8. Oil sorption capacity measurements of the MNP@DS material for different oils in 10 runs.

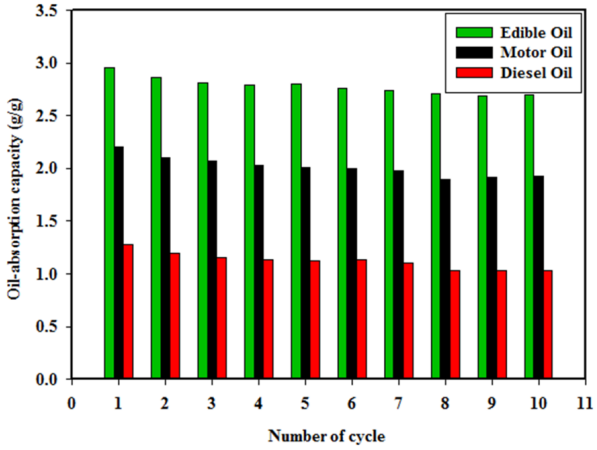

Figure 9. Oil sorption capacity measurements of the MNP@DO material for different oils in 10 runs.

possible to determine the organic loading of this material based on dodecyl sulfate moiety approximately, which was estimated to be 1.09 mmol.g^{-1}. For MNP@DO, the amount of grafted dodecanol was also evaluated using elemental analysis and it was estimated to be 1.13 mmol.g^{-1} according to the wt% of C (16.28%).

The BET method was carried out to determine the specific surface area and porosity of the adsorbents. The results are summarized in Table 1. As Table 1shows, the pore width was determined to be 10.61 nm and 8.22 nm for MNP@DO and MNP@DS, respectively. This experiment showed approximately the same surface area for both materials (112.4 m^2/g for MNP@DO and 117.1 m^2/g for MNP@DS).

3.2 Adsorption mechanism and oil absorbency of MNP@DO and MNP@DS

The remarkable oil adsorption capacity of MNP@DO and MNP@DS primarily arises from the exceptional porosity and hydrophobic nature of the sorbent materials. These materials exhibit significant potential for the effective removal of oil from water. Their nonmagnetic properties and hydrophobic surfaces make them particularly well-suited for this application. The water sorption tests presented in Figure 7 strongly support the magnetic nanoparticles' high affinity for adsorbing oil from the water's surface. Upon introducing both MNP@DO and MNP@DS materials into an oil-water mixture, the oil rapidly accumulates on the surface of the magnetic nanoparticles, while the sorbent material remains afloat on the water's surface – an ideal scenario for efficient removal. The utilization of an external magnetic field enables the straightforward retrieval of MNP@DO and MNP@DS materials from the water's surface. This possibility is highly important in designing mechanical machines such as skimmers in order to contentiously collect oil from water surface.

The oil sorption capacities of MNP@DS and MNP@DO catalysts are presented in Figures 8 and 9, respectively. The sorption tests employed three different types of oils: edible oil, motor oil, and diesel oil. The results reveal that MNP@DS exhibited a relatively lower sorption capacity of approximately 2.0 grams of oil per gram of the catalyst, depending on the type of oil. On the other hand, MNP@DO demonstrated more favorable sorption ability, nearing approximately 3.0 grams of oil per gram of catalyst. This slight difference in sorption capacity may be attributed to the polarity of the sulfonyl group within the structure of the grafted dodecyl sulfate on the MNPs' surface. Since the magnetic nanoparticles are not notably porous, the ability to absorb two or three times their own mass of oil can be attributed to the grafted organic layer on the surface of the MNPs. The carbon chains of dodecyl sulfate and dodecanol create this organic layer on the MNPs' surface, leading to van der Waals interactions between the organic chains of the oil and the grafted dodecyl chains on the MNPs' surface. The oil-removing ability was related to the lipophilicity of the surface of these nanomaterials, which mediated the aggregation of the oil molecules. In addition, the monodispersity of the nanomaterials causes them to be easily dispersed in the system to efficiently collect the oil molecules to aggregate. One of the high efficiencies of these materials is related to their nanostructure, which small amount of them create high surface area (Figure 10).

Additionally, the reusability of these materials was assessed

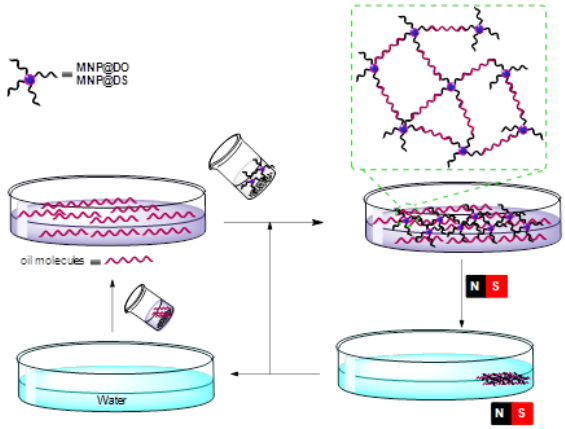

Figure 10. A schematic representation of the aggregation of oil particles and their removal from the surface of the water, mediated by magnetic nanomaterials.

(Figures 8 and 9), and they were found to be reusable for at least ten cycles without a significant decrease in adsorbent capacity. Therefore, it is possible to remove at least $2.0-3.0$ grams of oil per gram of the catalyst from water after ten uses, utilizing MNP@DO and MNP@DS catalysts, making them comparable to many other materials designed for oil removal from water surface. Considering the increasing rate of oil pollution of the seas, we need more research study in this field, and we anticipated that the magnetic sorbing nanomaterials has high potential and developing simple and efficient synthesis methods have many implications for the progress of this field.

4. Conclusion

Two magnetic sorbent catalysts comprised of magnetic nanoparticles and sodium dodecyl sulfate/ or dodecanol (MNP@DS and MNP@DO) were introduced and fabricated through a simple chemical process. The raw materials used for the preparation of these oil sorbent catalysts are readily available, cost-effective, and easily accessible. These materials were characterized using various analytical techniques, such as FT-IR, SEM, EDX, VSM, BET, and TGA-DTG. The oil sorption capacity of these magnetic sorbents was assessed in various oil-water mixtures to determine their efficacy in oil spillage treatment. The results reveal that MNP@DS exhibited a sorption capacity of approximately 2.0 g/g, depending on the type of oil, and MNP@DO demonstrate a more favorable sorption ability of about 3.0 g/g. The results of oil sorption tests demonstrated a substantial sorption capacity, with the ability to maintain effectiveness at $2.0-3.0$ g/g after 10 cycles of reuse for both materials across three different oil types. The excellent performance of these sorbent materials is attributed to the magnetic properties and hydrophobic surface characteristics resulting from the organic moieties grafted onto the magnetic nanoparticles. The organic layer on the surface of MNPs, cause van der Waals interactions between the organic chain of oil and grafted dodecyl chain on the MNPs surface. Overall, these findings suggest the considerable potential of these magnetic oil sorbent catalysts for environmental applications, particularly in the context of oil removal and separation from seawater surfaces.

Acknowledgments
This work was supported by Malek-Ashtar University of Technology, and the authors express their gratitude for the support provided.

Ethical Approval
This manuscript does not report on or involve the use of any animal or human data or tissue. So the ethical approval is not applicable.

Authors Contributions
Authors have equally contributed in preparing the paper.

Availability of Data and Materials
The data that support the findings of this study are available from the corresponding author upon reasonable request.

Conflict of Interests
The authors declare that they have no known competing financial interests or personal relationships that could have appeared to influence the work reported in this paper.

References

[1] L Yan, X Yang, Y Li, R Song, Y Lin, Q Huang, and L Shao. "Acid-resistant supramolecular nanofibrous hydrogel membrane with core-shell structure for highly efficient oil/water separation.". *J. Member. Sci.*, **679**:121705, 2023. DOI: https://doi.org/10.1016/j.memsci.2023.121705.

[2] J Gao, J Wang, M Cai, Q Xu, J Zhang, X Cao, J Zhang, and Y Chen. "Advanced superhydrophobic and multifunctional nanocellulose aerogels for oil/water separation: A review.". *Carbohydr. Polym.*, **300**:120242, 2022. DOI: https://doi.org/10.1016/j.carbpol.2022.120242.

[3] A Raj, RM Rego, KV Ajeya, HY Jung, TA, GM Neelgund, M Kigga, and MD Kurkuri. "Underwater oleophobic-super hydrophilic strontium-MOF for efficient oil/water separation.". *Chem. Eng. J.*, **453**:139757, 2023. DOI: https://doi.org/10.1016/j.cej.2022.139757.

[4] L Yan, X Yang, H Zeng, Y Zhao, Y Li, X He, J Ma, and L Shao. "Nanocomposite hydrogel engineered hierarchical membranes for efficient oil/water separation and heavy metal removal.". *Journal of Membrane Science*, **668**:121243, 2023. DOI: https://doi.org/10.1016/j.memsci.2022.121243.

[5] L Han, L Shen, H Lin, Zh Huang, Y Xu, R Li, B Li, Ch Chen, W Yu, and J Teng. "3D printing titanium dioxide-acrylonitrile-butadiene-styrene (TiO_2-ABS) composite membrane for efficient oil/water separation.". *Chemosphere*, **315**:137791, 2023. DOI: https://doi.org/10.1016/j.chemosphere.2023.137791.

[6] P Zhang, Z He, X Luo, Z Jia, and L He. "Optimization of graphene oxide modified mesh for separation of O/W emulsions.". *Chemical Engineering Science*, **270**:118543, 2023. DOI: https://doi.org/10.1016/j.ces.2023.118543.

[7] QF Wei, RR Mather, AF Fotheringham, and RD Yang. "Evaluation of nonwoven polypropylene oil sorbents in marine oil-spill recovery". *Marine Pollution Bulletin*, **46**(6):780–783, 2003. DOI: https://doi.org/10.1016/S0025-326X(03)00042-0.

[8] JS Amin, MV Abkenar, and S. Zendehboudi. "Natural sorbent for oil spill cleanup from water surface: environmental implication.". *Industrial & Engineering Chemistry Research*, **54**(43):10615–10621, 2015. DOI: https://doi.org/10.1021/acs.iecr.5b01715.

[9] Q Wen, J Di, L Jiang, J Yu, and R Xu. "Zeolite-coated mesh film for efficient oil–water separation.". *Chemical Science*, **4**:591–595, 2013. DOI: https://doi.org/10.1039/C2SC21772D.

[10] RK Gupta, GJ Dunderdale, MW England, and A Hozumi. "Oil/water separation techniques: a review of recent progresses and future directions.". *Journal of Materials Chemistry A*, **5**:16025–16058, 2017. DOI: https://doi.org/10.1039/C7TA02070H.

[11] N Zhang, Y Qi, Y Zhang, J Luo, P Cui, and W Jiang. "A review on oil/water mixture separation material.". *Industrial & Engineering Chemistry Research*, **59**:14546–14568, 2020. DOI: https://doi.org/10.1021/acs.iecr.0c02524.

[12] Q He, Zh Guo, S Ma, and Zh He. "Recent advances in superhydrophobic papers for oil/water separation: a mini-review.". *ACS Omega*, **7**(48):43330–43336, 2022. DOI: https://doi.org/10.1021/acsomega.2c05886.

[13] J Fritt-Rasmussen, PJ Brandvik, A Villumsen, and EH Stenby. "Comparing ignitability for in situ burning of oil spills for an asphaltenic, a waxy and a light crude oil as a function of weathering conditions under arctic conditions.". *Cold Regions Science and Technology*, **72**:1–6, 2012. DOI: https://doi.org/10.1016/j.coldregions.2011.12.001.

[14] V Rajakovic, G Aleksic, M Radetic, and L Rajakovic. "Efficiency of oil removal from real wastewater with different sorbent materials.". *Journal of Hazardous Materials*, **143**:494–499, 2007. DOI: https://doi.org/10.1016/j.jhazmat.2006.09.060.

[15] M Ghorbani, MH Vakili, and E Ameri. "Fabrication and evaluation of a biopolymer-based nanocomposite membrane for oily wastewater treatment.". *Materials Today Communications*, **28**:102560, 2021. DOI: https://doi.org/10.1016/j.mtcomm.2021.102560.

[16] Zh Xue, Y Cao, N Liu, L Feng, and L Jiang. "Special wettable materials for oil/water separation". *Journal of Materials Chemistry A*, **2**:2445–2460, 2014. DOI: https://doi.org/10.1039/C3TA13397D.

[17] J Ge, H-Y Zhao, H-W Zhu, J Huang, L-A Shi, and S-H Yu. "Advanced sorbents for oil-spill cleanup: recent advances and future perspectives.". *Advanced Materials*, **28**(47):10459–10490, 2016. DOI: https://doi.org/10.1002/adma.201601812.

[18] GO Aydin and HB Sonmez. "Organic–inorganic hybrid gels for the selective absorption of oils from water.". *Environmental Science and Pollution Research*, **23**:11695–11707, 2016. DOI: https://doi.org/10.1007/s11356-016-6342-9.

[19] AO Ifelebuegu and A Johnson. "Nonconventional low-cost cellulose- and keratin-based biopolymeric sorbents for oil/water separation and spill cleanup: a review.". *Critical Reviews in Environmental Science and Technology*, **47**:964–1001, 2017. DOI: https://doi.org/10.1080/10643389.2017.1318620.

[20] J Mao, W Jiang, J Gu, S Zhou, Y Lu, and T Xie. "Synthesis of P (St-DVB)/Fe_3O_4 microspheres and application for oil removal in aqueous environment.". *Applied Surface Science*, **317**:787–793, 2014. DOI: https://doi.org/10.1016/j.apsusc.2014.08.191.

[21] S Zhou, W Jiang, T Wang, and Y Lu. "Highly hydrophobic, compressible, and magnetic polystyrene/Fe_3O_4/graphene aerogel composite for oil–water separation.". *Industrial & Engineering Chemistry Research*, **54**(20):5460–5467, 2015. DOI: https://doi.org/10.1021/acs.iecr.5b00296.

[22] NN Nassar, A Hassan, and P Pereira-Almao. "Application of nanotechnology for heavy oil upgrading: catalytic steam gasification/cracking of asphaltenes.". *Energy Fuels*, **25**(4):1566–1570, 2011. DOI: https://doi.org/10.1021/ef2001772.

[23] Zh Jiang, LD Tijing, A Amarjargal, CH Park, K-J An, HK Shon, and CS Kim. "Removal of oil from water using magnetic bicomponent composite nanofibers fabricated by electrospinning.". *Composites Part B: Engineering*, **77**:311–318, 2015. DOI: https://doi.org/10.1016/j.compositesb.2015.03.067.

[24] L Wu, L Li, B Li, J Zhang, and A Wang. "Magnetic, durable, and superhydrophobic Polyurethane@Fe_3O_4@SiO_2@Fluoropolymer sponges for selective oil absorption and oil/water separation.". *ACS Applied Materials & Interfaces*, **7**(8):4936–4946, 2015. DOI: https://doi.org/10.1021/am5091353.

[25] R Du, Q Zhao, P Li, H Ren, X Gao, and J Zhang. "Ultrathermostable, magnetic-driven, and superhydrophobic quartz fibers for water remediation". *ACS Applied Materials & Interfaces*, **8**(1):1025–1032, 2016. DOI: https://doi.org/10.1021/acsami.5b11341.

[26] Z Azizi Haghighat and E Ameri. "Synthesis and characterization of nano magnetic wheat straw for lead adsorption.". *Desalination and Water Treatment*, **57**(21):9813–9823, 2016. DOI: https://doi.org/10.1080/19443994.2015.1033475.

[27] R Fareghi-Alamdari, M Golestanzadeh, and N Zekri. "Application of nanosized $Cu_{0.5}Co_{0.5}Fe_2O_4$ Spinel Ferrite as a Nanocatalyst in the Synthesis of 14-Aryl-14H-dibenzo[a,j]xanthene derivatives under solvent-free conditions.". *Journal of the Chinese Chemical Society*, **61**(12):1341–1350, 2014. DOI: https://doi.org/10.1002/jccs.201400148.

[28] R Fareghi-Alamdari, N Zekri, and F Mansouri. "Enhancement of catalytic activity in the synthesis of 2-amino-4H-chromene derivatives using both copper- and cobalt-incorporated magnetic ferrite nanoparticles.". *Research on Chemical Intermediates*, **43**:6537–6551, 2017. DOI: https://doi.org/10.1007/s11164-017-3003-7.

[29] R Fareghi-Alamdari, M Nadiri Niri, H Hazarkhani, and N Zekri. "Diacidic ionic liquid supported on magnetic-silica nanocomposite: a novel, stable, and reusable catalyst for selective diester production.". *Journal of the Iranian Chemical Society*, **15**:2615–2629, 2018. DOI: https://doi.org/10.1007/s13738-018-1450-8.

[30] R Fareghi-Alamdari, MS Saeedi, and F Panahi. "New bis(N-heterocyclic carbene) palladium complex immobilized on magnetic nanoparticles: as a magnetic reusable catalyst in Suzuki-Miyaura cross coupling reaction.". *Applied Organometallic Chemistry*, **31**(12):e3870, 2017. DOI: https://doi.org/10.1002/aoc.3870.

[31] A Khalafi-Nezhad, M Nourisefat, and F Panahi. "L-Cysteine functionalized magnetic nanoparticles (LCMNP): a novel magnetically separable organocatalyst for one-pot synthesis of 2-amino-4H-chromene-3-carbonitriles in water.". *Organic & Biomolecular Chemistry*, **13**:7772–7779, 2015. DOI: https://doi.org/10.1039/C5OB01030F.

[32] A Khalafi-Nezhad, S Mowlazadeh Haghighi, and F Panahi. "Nano-TiO_2 on dodecyl-sulfated silica: as an efficient heterogeneous lewis acid–surfactant-combined catalyst (HLASC) for reaction in aqueous media.". *ACS Sustainable Chemistry & Engineering*, **1**:1015–1023, 2013. DOI: https://doi.org/10.1021/sc4000913.

[33] A Khalafi-Nezhad, M Divar, and F Panahi. "Magnetic nanoparticles-supported tungstic acid (MNP-TA): an efficient magnetic recyclable catalyst for the one-pot synthesis of spirooxindoles in water.". *RSC Advances*, **5**(3):2223–2230, 2015. DOI: https://doi.org/10.1039/C4RA12976H.